CHAPTER 12

The hypothetical amyloid transformation of transthyretin

Mateusz Banach[1], **Leszek Konieczny**[2], **Irena Roterman**[1]
[1]Department of Bioinformatics and Telemedicine, Jagiellonian University – Medical College, Krakow, Poland
[2]Chair of Medical Biochemistry, Jagiellonian University – Medical College, Krakow, Poland

Contents

References 239

Conceptual diagram presenting linear propagation of (gray) bands with varying hydrophobicity. If this linear pattern is joined by fragments marked in red (initially not fitting to linear propagation), the protein is at risk of undergoing amyloid transformation.

If we accept the presented amyloid identification criteria as accurate, we may apply them to predict the structures of various amyloids – including the transthyretin amyloid. The structure of this protein is listed in PDB under ID 1DVQ [1], in its dimeric form, with each chain consisting of residues 10–124. Its structure is characterized as a mainly β-sandwich (CATH code 2.60.40.180). Each β-sheet consists of four antiparallel β-strands. In addition, a single helical fragment is also present (residues 74–81).

Fig. 12.1 illustrates the distributions of hydrophobicity (T, O and H) as it appears in both chains treated as parts of dimer and as individual structural units. The aim of Fig. 12.1 is to visualize the relation between T and O as well as between O and H, with some fragments exhibiting strong alignment between the observed and intrinsic distributions. The two chains appear almost identical in terms of all three distributions.

From Globular Proteins to Amyloids
ISBN: 978-0-08-102981-7
https://doi.org/10.1016/B978-0-08-102981-7.00020-8

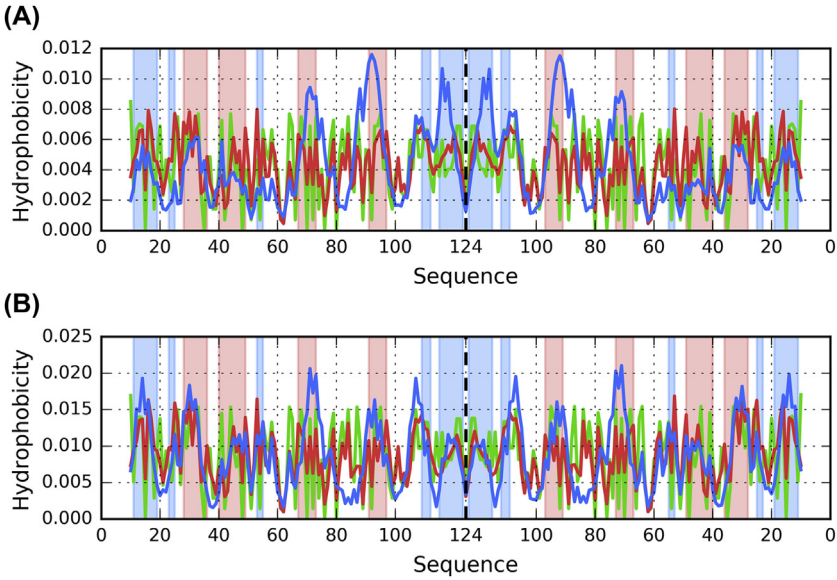

Fig. 12.1 Theoretical (T, blue) and observed (O, red) hydrophobicity distribution profiles for transthyretin dimer (1DVQ) chains A and B (A) treated as part of the dimer. (B) treated as individual units.

Thick dashed line at position 124 separates chain A (left) from chain B (right). To reproduce the symmetry of the complex, results for chain B are present in reverse order. Components of the appropriate β-sheets are marked by red (starting strand 28−36, called also as II) and blue (starting strand 11−19, called also as I) backgrounds.

Clearly, the structure lacks a prominent hydrophobic core (Fig. 12.1 and Table 12.1). The RD (T-O-R) higher than 0.5 expresses the lack of centric hydrophobic core. The RD (T-O-H) below 0.5 suggests not significant influence of intrinsic hydrophobicity. However the highest correlation coefficient for HvO relation suggest the strong influence of intrinsic hydrophobicity on the final distribution. The lack of centric hydrophobic core seems to be caused mainly by the fragments at 60−80, 80−100 and 100−120 (Fig. 12.1). Additionally, as suggested by the arrangement of β-strands, it appears that the initial β-strand at 11−19 (marked on Fig. 12.1 by blue background) is closer to the theoretical distribution whereas the strand at 28−36 (red background on Fig. 12.1) is more discordant. This observation is supported by the parameters listed in Table 12.1, where the β-sheet 28−36 (the starting fragment used to identify this sheet)

Table 12.1 Fuzzy oil drop parameters (RD values and correlation coefficients) for transthyretin (1DVQ): dimer, chains treated as parts of dimer, chains treated as individual units and β-sheets comprising the dimer (with status of β-strands as they appear in those sheets). Values given in bold identify discordance (RD > 0.5) and positions with large disproportion of correlation coefficient.

Trans thyretin (1DVQ)	Fragment	RD		Correlation coefficient		
		T-O-R	T-O-H	HvT	TvO	HvO
Dimer	A + B	**0.650**	0.467	**0.222**	**0.368**	**0.722**
	Chain A in dimer	**0.652**	0.467	**0.225**	**0.352**	**0.723**
	Chain B in dimer	**0.648**	0.468	**0.220**	**0.380**	**0.720**
	Chain A individual	**0.562**	0.370	0.328	0.592	0.687
	Chain B individual	**0.556**	0.368	0.317	0.591	0.687
β-strands						
	11–19	0.440	0.089	0.589	0.557	0.853
	23–25 + 53–55	0.411	0.343	0.682	0.602	0.751
	104–112	0.148	0.184	0.677	0.910	0.586
	115–123	**0.639**	**0.697**	0.054	0.576	0.568
β-sheet I		**0.717**	0.444	0.251	0.274	0.582
β-strands						
	28–36	0.467	0.171	0.468	0.489	0.872
	40–49	**0.517**	0.216	0.713	0.155	0.533
	67–73	**0.760**	0.182	**−0.263**	**−0.549**	**0.898**
	91–97	**0.776**	**0.704**	**−0.090**	**−0.423**	**0.897**
β-sheet II		**0.682**	0.326	**0.162**	**0.144**	**0.764**

appears to be strongly dominated by the intrinsic hydrophobicity of its component residues.

In search for fragments representing status recognized as amyloidogenic (Chapter 10), the profile of correlation coefficients (for 5 aa window) is presented in Fig. 12.2. Based on the description and applicability of the fuzzy oil drop model discussed in previous chapters, we may draw conclusions regarding the propensity of the presented structures to undergo amyloid transformation. This process is aided by identifying sections where the observed distribution deviates from the theoretical distribution in specific ways. We therefore calculate correlation coefficients for consecutive 5 aa fragments (using an overlapping moving frame), seeking fragments which exhibit low (preferably negative) values of HvT and TvO, coupled with

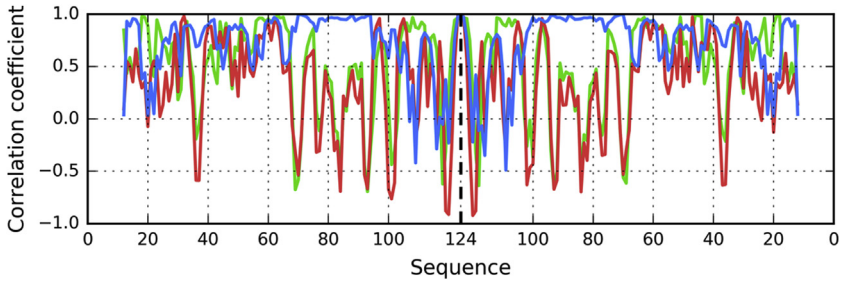

Fig. 12.2 Correlation coefficients between FOD hydrophobicity profiles calculated for transthyretin dimer (1DVQ) in 5 aa overlapping moving frame mode: HvO – blue, HvT – red, TvO – green. Thick dashed line at position 124 separates chain A (left) from chain B (right). To reproduce the symmetry of the complex, results for chain B are present in reverse order. This diagram enables us to identify amyloid transformation seeds (positions with disproportionally high HvO values vs. low HvT and TvO values).

high values of HvO. Fig. 12.2 shows the variability of correlation coefficients computed for each β-sheet in transthyretin.

Based on the chart shown in Fig. 12.2, the following fragments are seen to fulfill all amyloid identification criteria: 34–45, 66–69, 73–75, 80–84, 89–93 and 98–102 (in each chain). To better visualize the structural specificity, the correlation coefficients limited to β-sheets following the spatial localization of certain polypeptide chain fragments is shown in Fig. 12.3.

Ordering of residues is consistent with their respective placement in the dimer (antiparallel arrangement). To avoid displaying multiple gaps between the strands, results are conflated into contiguous sequences, hence no exact numbering is marked on the horizontal axis.

Blue – HvO, red-TvO, green HvT.

Focusing the analysis on the status of β-sheets expressed by hydrophobicity profile correlation coefficients provides an unobstructed view of differences between those fragments. In the presented diagram (Fig. 12.3), amino acid sequences are ordered in accordance with the supersecondary structure of the dimer (this particularly concerns the ordering of β-strands in β-sheets). For this structure we calculate correlation coefficients using a 5 aa moving frame for β-sheets (treating them as the independent structural unit). The results (Fig. 12.3) reveal significant variability of β-sheets which make up the β-sandwich.

The sheet identified as "11–19" (I) does not appear to satisfy our amyloid identification criteria (Fig. 12.3B), whereas the sheet identified as

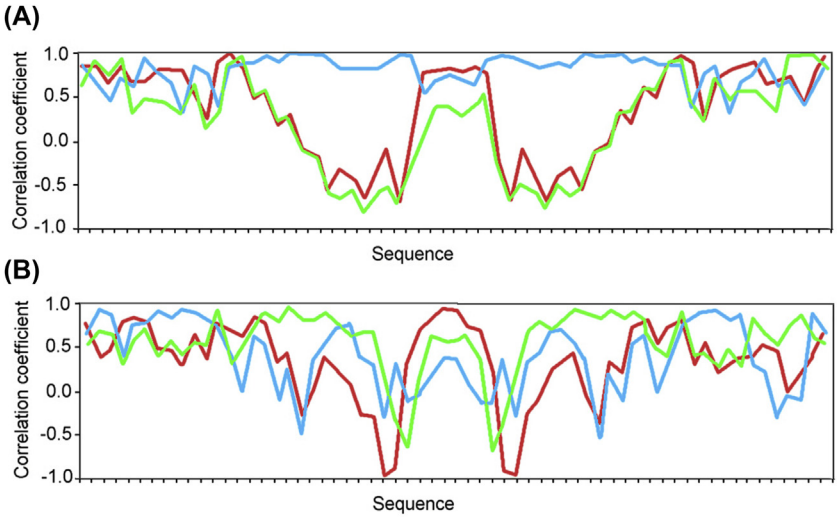

Fig. 12.3 Correlation coefficients between FOD hydrophobicity profiles calculated for β-sheets in transthyretin dimer (1DVQ) in 5-aa overlapping moving frame mode. (A) profile for β-sheet I (starting fragment 11−19). (B) profile for β-sheet II (starting fragment 28−36).

"28−36" (II) reveals strong involvement of fragments in which the observed distribution deviates from T in favor of H (Fig. 12.3A). Terminal residues (i.e. the initial and final fragments shown in Fig. 12.3A) are generally accordant with T. These residues correspond to the fragment at 40−49, which occupies an outlying location in the β-sheet. The fragments at 67−73 and 91−97 exhibit nonuniform correlation coefficients, (central section in Fig. 12.3A, showing negative values of HvT and TvO).

Assembling all the previously mentioned fragments (colored red in Fig. 12.4) identifies part of the β-sheet which − according to FOD based parameters − represents amyloid-like status. The loops (blue on Fig. 12.4) do not exhibit linear propagation of bands of different hydrophobicity. However if these two loops change their orientation versus the amyloid-like fragment of β-sheet, and continue the profile making it similar to the red fragment, the possible propagation in both directions appears to be possible.

It can be surmised that the fragments identified in the analysis of charts plotted in Fig. 12.3B act as amyloid seeds, since their spatial arrangement is already characteristic of a linear pattern. When joined by additional fragments (colored red) which do not belong to the β-sandwich, this pattern

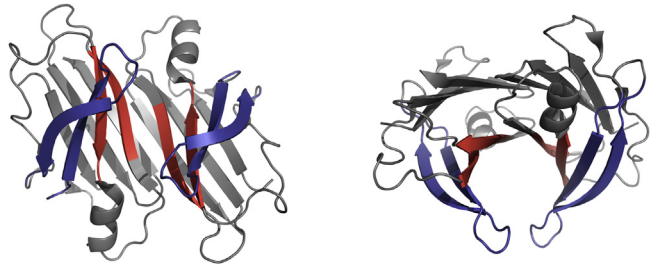

Fig. 12.4 3D presentation of transthyretin dimer (1DVQ) from two angles. Red fragments (67—73, 91—97, in each chain) express negative values of HvT and TvO, along with strongly positive values of HvO. Fragments 27—50 in each chain (shown in blue) are expected to undergo structural rearrangement in the process of amyloid transformation, aligning themselves with the existing linear pattern exhibited by other strands of β-sheet II.

spreads to the entire dimer. It also creates an open-ended structure which may attach itself to similarly arranged fragments in another dimer (and so on), ultimately producing a fibrillar structure. The structure illustrated in Fig. 12.5 also clearly shows a twist, which is characteristic of a fibril. Additional units (in this case — dimers) are complexed at an angle, resulting in a twisted structure.

Based on the presented correlation coefficients we may speculate that in the amyloid form of transthryretin residues 40—49 along with the entire fragment at 27—50 should adopt a linear structural pattern with other strands comprising β-sheet II. Such arrangement (which, of course, calls for additional conformational changes) may provide the necessary conditions for further propagation of the amyloid.

A similar structure, based on structural analysis of immunoglobulin light chain domain VL (relatively easy to undergo the amyloid transformation), has been proposed in Ref. [2]. While it differs somewhat to the one shown above, it also demonstrates the necessary conditions for further linear propagation in the event of certain rearrangements within the dimer. In this specific case, a bend in the fragment at 27—50 would enable it to align itself with the planar β-structure, facilitating further propagation of the observed discordance between T and O and preventing the dimer from forming a hydrophobic core.

Number of papers discussing transthyretin amyloid transformation is very large [3—17]. Among them are many of experimental character. Some of them discuss the possible therapeutic treatments [18—22].

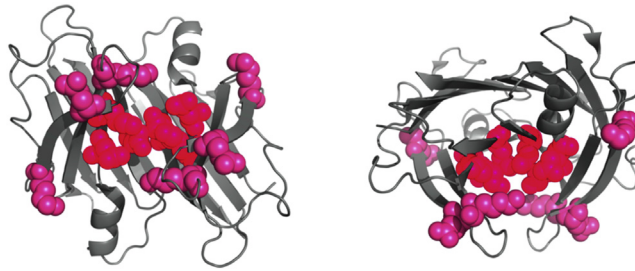

Fig. 12.5 3D presentation of transthyretin dimer (1DVQ) from two angles with residues forming a linear propagation of hydrophobicity distinguished in red (70, 72, 92) and residues exhibiting similar hydrophobic characteristics (low hydrophobicity with neighbors of higher hydrophobicity) distinguished in blue (35, 42 and 48). If the strands in 27–50 residue range (colored blue in Fig. 12.4) change the orientation to participate in linear propagation of low hydrophobicity band together with residues given in Fig. 12.4 in red, the unlimited propagation of bands of low and higher hydrophobicity bands on both sites (and thus amyloid formation) becomes possible.

References

[1] Klabunde T, Petrassi HM, Oza VB, Raman P, Kelly JW, Sacchettini JC. Rational design of potent human transthyretin amyloid disease inhibitors. Nature Structural Biology 2000;7(4):312–21. https://doi.org/10.1038/74082.

[2] Banach M, Kalinowska B, Konieczny L, Roterman I. Possible mechanism of amyloidogenesis of V domains. Self-Assembled Molecules – New Kind of Protein Ligands 2017:77–100. https://doi.org/10.1007/978-3-319-65639-7_5.

[3] Colon W, Kelly JW. Partial denaturation of transthyretin is sufficient for amyloid fibril formation in vitro. Biochemistry 1992;31(36):8654–60. https://doi.org/10.1021/bi00151a036.

[4] Connelly S, Choi S, Johnson SM, Kelly JW, Wilson IA. Structure-based design of kinetic stabilizers that ameliorate the transthyretin amyloidoses. Current Opinion in Structural Biology 2010;20(1):54–62. https://doi.org/10.1016/j.sbi.2009.12.009.

[5] Foss TR, Wiseman RL, Kelly JW. The pathway by which the tetrameric protein transthyretin dissociates. Biochemistry 2005;44(47):15525–33. https://doi.org/10.1021/bi051608t.

[6] Hurshman AR, White JT, Powers ET, Kelly JW. Transthyretin aggregation under partially denaturing conditions is a downhill polymerization. Biochemistry 2004;43(23):7365–81. https://doi.org/10.1021/bi049621l.

[7] Kelly JW. The alternative conformations of amyloidogenic proteins and their multistep assembly pathways. Current Opinion in Structural Biology 1998;8(1):101–6. https://doi.org/10.1016/s0959-440x(98)80016-x.

[8] Kelly JW. Amyloid fibril formation and protein misassembly: a structural quest for insights into amyloid and prion diseases. Structure 1997;5(5):595–600. https://doi.org/10.1016/s0969-2126(97)00215-3.

[9] Kelly J, Colon W, Lai Z, Lashuel H, Mcculloch J, Mccutchen S, Peterson S. Transthyretin quaternary and tertiary structural changes facilitate misassembly into amyloid. Advances in Protein Chemistry 1997;50:161–81. https://doi.org/10.1016/s0065-3233(08)60321-6.

[10] Kelly JW. Alternative conformations of amyloidogenic proteins govern their behavior. Current Opinion in Structural Biology 1996;6(1):11–7. https://doi.org/10.1016/s0959-440x(96)80089-3.
[11] Knowles TPJ, Vendruscolo M, Dobson CM. The amyloid state and its association with protein misfolding diseases. Nature Reviews Molecular Cell Biology 2014;15(6):384–96. https://doi.org/10.1038/nrm3810.
[12] Lim KH, Dasari AKR, Hung I, Gan Z, Kelly JW, Wemmer DE. Structural changes associated with transthyretin misfolding and amyloid formation revealed by solution and solid-state NMR. Biochemistry 2016;55(13):1941–4. https://doi.org/10.1021/acs.biochem.6b00164.
[13] Lim KH, Dasari AKR, Ma R, Hung I, Gan Z, Kelly JW, Fitzgerald MC. Pathogenic mutations induce partial structural changes in the native β-sheet structure of transthyretin and accelerate aggregation. Biochemistry 2017;56(36):4808–18. https://doi.org/10.1021/acs.biochem.7b00658.
[14] Palaninathan SK, Mohamedmohaideen NN, Snee WC, Kelly JW, Sacchettini JC. Structural insight into pH-induced conformational changes within the native human transthyretin tetramer. Journal of Molecular Biology 2008;382(5):1157–67. https://doi.org/10.1016/j.jmb.2008.07.029.
[15] Saelices L, Chung K, Lee JH, Cohn W, Whitelegge JP, Benson MD, Eisenberg DS. Amyloid seeding of transthyretin by ex vivo cardiac fibrils and its inhibition. Proceedings of the National Academy of Sciences of the United States of America 2018;115(29):E6741–50. https://doi.org/10.1073/pnas.1805131115.
[16] Saelices L, Sievers SA, Sawaya MR, Eisenberg DS. Crystal structures of amyloidogenic segments of human transthyretin. Protein Science 2018;27(7):1295–303. https://doi.org/10.1002/pro.3420.
[17] Dasari AKR, Hung I, Gan Z, Lim KH. Two distinct aggregation pathways in transthyretin misfolding and amyloid formation. Biochimica et Biophysica Acta (BBA) – Proteins & Proteomics 2018. https://doi.org/10.1016/j.bbapap.2018.10.013. pii: S1570-9639(18)30188-2.
[18] Ankarcrona M, Winblad B, Monteiro C, Fearns C, Powers ET, Johansson J, Kelly JW. Current and future treatment of amyloid diseases. Journal of Internal Medicine 2016;280(2):177–202. https://doi.org/10.1111/joim.12506.
[19] Balch WE, Morimoto RI, Dillin A, Kelly JW. Adapting proteostasis for disease intervention. Science 2008;319(5865):916–9. https://doi.org/10.1126/science.1141448.
[20] Coelho T, Merlini G, Bulawa CE, Fleming JA, Judge DP, Kelly JW, Huertas P. Mechanism of action and clinical application of tafamidis in hereditary transthyretin amyloidosis. Neurology and Therapy 2016;5(1):1–25. https://doi.org/10.1007/s40120-016-0040-x.
[21] Eisele YS, Monteiro C, Fearns C, Encalada SE, Wiseman RL, Powers ET, Kelly JW. Targeting protein aggregation for the treatment of degenerative diseases. Nature Reviews Drug Discovery 2015;14(11):759–80. https://doi.org/10.1038/nrd4593.
[22] Schonhoft JD, Monteiro C, Plate L, Eisele YS, Kelly JM, Boland D, Kelly JW. Peptide probes detect misfolded transthyretin oligomers in plasma of hereditary amyloidosis patients. Science Translational Medicine 2017;9(407). https://doi.org/10.1126/scitranslmed.aam7621.